SAND--89-1192C

CONF-890632--1

DE89 013155

A FULLY AUTOMATED, SINGLE-CONNECTION TESTER FOR T/R MODULES

George R. Sloan and James M. Simons
Sandia National Laboratories
Albuquerque, NM

Introduction

An inherent aspect of active array radars is the use of large numbers-- typically hundreds-- of transmit/receive (T/R) modules. The implementation of this technology at Sandia has created new challenges for the tester designer. Foremost among these challenges is the need to design T/R module testers which can accommodate such large numbers of devices-under-test (DUTs). This task is complicated by the fact that state-of-the-art T/R modules are extremely sophisticated and require a broad spectrum of tests for adequate evaluation.

The Sandia T/R module operates in Ku band and consists of a transmitter (2 W MMIC amplifier), receiver (LNA), programmable phase shifter, programmable attenuator, modulator, switched limiter, and gate-array controller. The programmable phase shifter is common to both the transmitter and receiver, but the attenuator is unique to the receiver. The general types of measurements and tests needed to evaluate the module include (1) gain/peak-power measurements, (2) phase accuracy, (3) phase linearity, (4) pulse fidelity/response, (5) load/source-pulls, (6) receiver noise figure, (7) receiver linearity, and (8) jamming environment survivability. The instruments required for the above tests include a network analyzer, a spectrum analyzer, a noise figure meter, a peak-power meter, and an automated tuner system. The key to a successful tester is in integrating all of the above instruments such that the desired measurements can all be performed from a single, two-port, tester-to-DUT connection. The natural consequence of such a design is that some measurements will have to be de-embedded from the integrated test setup. This paper addresses both the tester's instrument integration and the resulting de-embedding concerns.

Instrument Integration

The "heart" of the Sandia tester is an HP 8510, pulsed-mode automatic network analyzer (ANA). The instrument's ability to measure pulsed-stimulus S-parameters is essential to T/R module testing because it allows the module to be accurately evaluated under real-world signal conditions. The 8510's new pulsed-mode capability can operate not only in the traditional frequency domain, but also in a new "pulse-profiling" time domain. This pulse-profiling capability actually allows the tester to analyze how the module's gain and phase response vary across a pulse. This information on transient response, especially for phase, is critical in evaluating whether the final active array radar can meet resolution specifications.

The new ANA is also the key to the tester's single-connection capability: The 85110A pulsed-mode test set includes special rear panel signal access links that make it especially amenable to integration with other instruments. These access links occur after the test set's forward/reverse (F/R) switch, but before its signal separation couplers. This is an ideal location for such ports because (1) placing them after the F/R switch means any signal modifications will occur only to one measurement port, and (2) placing them prior to the signal separation couplers means that any signal modifications will have only a minimal effect on ANA calibrations and accuracy. The Sandia tester uses these access links both for signal amplification and for integrating ancillary instruments with the ANA. In essence, the rear access links allowed the tester to essentially be built around the ANA's test set.

Unfortunately, the test-set integration scheme does have one drawback. The problem is simply that the ANA's test signal is not flat over frequency: over the module's test bandwidth (14.5 to 15.5 GHz), the drive signal was found to have about 1.5 dB of rolloff and 0.75 dB of ripple. This is not acceptable when making transmitter gain/phase measurements because the transmitter operates at or near compression; thus, both its gain and phase response are a function of the input signal level. Consequently, any swept gain/phase measurements on the transmitter would be corrupted by variations in the level of the test signal.

The solution to the above dilemma is simply to externally level the ANA for S_{21} measurements. A little known feature of the 8510 is that it can take advantage of the HP 8341B's crystal leveling capability. Ideally, the leveling should occur as close to the DUT as possible. However, because most of the signal variation is due to the F/R switch, leveling at the access link will clear up most of the variation at the DUT port. Unfortunately, the external leveling creates its own unwanted side-effect: A full two-port error correction/calibration is no longer possible when the leveling is in effect. (This is because two-port error correction requires bi-directional measurements.) The solution to this side-effect is simply to use one-port/response calibrations for the transmitter measurements. The accuracy lost in using a simple response calibration for S_{21} measurements is negligible for a well matched, high gain, high isolation device, which are all characteristics of the T/R module transmitter.

Figure 1 shows a block diagram of the test set and its interconnections to the other instruments of the tester. The majority of the block diagram is self-explanatory; however, the following explanation is included to provide the reader with a guided tour of the instrument integration.

First, note that the access links incorporate dual transfer switches. One purpose of these switches is to give the tester the capability of switching in/out all of the access port

modifications when desired. In other words, the transfer switches allow the ANA to easily revert to an unmodified, stand-alone state when the operator desires. The other purpose for the switches is to switch in/out the noise figure measurement system. Note that with the noise source at port 2 and the meter connection at port 1, the system is configured for receiver measurements. In addition to the dual switches, port 2 incorporates a high power switch to provide access to the jammer (TWT amplifier). The additional switch is necessary due to the TWT's high output power.

Channel 1 and channel 2 of the peak-power meter are coupled into the test set's path via 20 dB couplers at both access links. Peak-power measurements are only intended to be made on the transmitter channel of the T/R module: Note that the configuration illustrated by the block diagram allows channel 1 to measure transmitter input power, while channel two is set up to measure transmitter output power. This configuration allows the tester to accurately control the input power level to the radar port, and it is ideal for making gain compression measurements. In addition, it allows the tester to examine pulse fidelity parameters (i.e., rise and fall times) both before and after the DUT. The 20 Db coupling factor on both ports assures that both the input and output signals are within the acceptable power meter measurement range.

The obvious purpose for the amplifier in the port 1 access link is to boost the ANA's signal to the needed transmitter drive level. The circulator following the amplifier both isolates the ANA signal from the amplifier's mismatch and directs the receiver's output signal to the spectrum analyzer, instead of to the amplifier. The corresponding circulator in the port 2 access link similarly directs the transmitter's output signal to the spectrum analyzer, but it also protects the F/R switch from the transmitter's high power output signal. (The damage level for the F/R switch is only 20 dBm, but the rest of the test set can handle up to 43 dBm.)

The second coupler in the port 2 access link is used in the creation of a two-tone signal for evaluation of the receiver's linearity (intermodulation/harmonic distortion analysis). Note that source 2 serves not only as part of the two-tone signal, but also as the LO for the ANA's and noise figure meter's test sets.

The automated tuners are placed just prior to the DUT. The tuner-to-DUT connection requires special consideration because even a small amount of loss in this connection can seriously degrade the SWR the tuner presents to the DUT. For this reason, the leveling coupler is placed on the ANA side of the tuner. The Maury tuners were chosen for use in the tester because they are of the slotted line genre; thus, when not involved in a load pull, the tuner's probe can be removed such that the tuner reverts to a low loss, 50 Ω transmission line. This capability is essential in integrating a load-pull capability into the single-connection tester concept.

Measurement De-Embedding

A natural consequence of the tester's single-connection capability is that the reference planes for peak-power and noise figure measurements are no longer at the DUT level. Thus, both peak-power and noise figure measurements will have to be de-embedded, meaning that the effects of pre- and post-DUT loss will have to be removed from the measurement results. The de-embedding process involves accurately characterizing the loss networks via full two-port S-parameter measurements and then using this characterization to calculate the correct de-embedding factor. The de-embedding expressions can be formulated in terms of S-parameters by utilizing the established technique of first defining an S-parameter flow diagram for the network, then defining the desired transfer function, and lastly, deriving the transfer function via Mason's loop rule.

Peak-Power Measurement De-Embedding

To de-embed the peak-power measurements, the tester must mathematically transfer the reference plane of the measurement from the coupler to the DUT. Channel 2 of the peak-power meter is used to measure the transmitter's output power; de-embedding this measurement is analogous to replacing the output tuner with a power meter that has an SWR identical to that of the tuner. In essence, the de-embedding factor is a classic two-port power gain measurement, and is defined as the ratio of the power delivered to the tuner to the power delivered to the power meter. (The key word in the definition is "delivered", which distinguishes true power gain from available gain, insertion gain, and transducer gain.) On the other hand, channel 1, which is used to measure the input power to the transmitter, has a de-embedding factor which is defined as the ratio of the power delivered to the DUT to the power delivered to the power meter. However, unlike the channel 2 measurement, there is no direct path between the DUT and the power meter; thus, this power gain measurement must be made from a three-port perspective.

Two-port de-embedding. Figure 2(a) illustrates the S-parameter flow graph of a two-port network. Applying the flow diagram to the channel 1 de-embedding loss, port 2 would correspond to the power-meter port, and port 1 would correspond to the DUT's antenna port. Applying Mason's technique, the desired power ratio is found to be

$$\frac{P_1}{P_2} = \frac{|1-\Gamma_L S_{22}|^2 - |S_{11}(1-\Gamma_L S_{22})+S_{21}\Gamma_L S_{12}|^2}{|S_{21}|^2(1-|\Gamma_L|^2)} \qquad (1)$$

The above equation is an exact expression for the de-embedding of peak-power measurements through a two-port network. Unfortunately, (1) is somewhat cumbersome to use for de-embedding during load pulls because all of the above S-parameters are a function of the tuner's position. However, the expression does lend itself to more workable approximations. First, note that if

the loss network has sufficient attenuation ($S_{21} \cdot S_{12}$ is small) and a good output return loss (S_{22} is small), then (1) reduces to

$$\frac{P_1}{P_2} = \frac{1-|S_{11}|^2}{|S_{21}|^2(1-|\Gamma_L|^2)} \tag{2}$$

Next, note that if the power meter reflection coefficient, Γ_L, is sufficiently small, then both (1) and (2) reduce to

$$\frac{P_1}{P_2} = \frac{1-|S_{11}|^2}{|S_{21}|^2} \tag{3}$$

Besides the obvious simplification, these approximations are especially advantageous for tuner de-embedding because they contain only parameter magnitudes, which ideally, do not vary over a constant-SWR pull. The attenuation requirement for (2) is easily satisfied due to the coupler loss, but the approximation of (3) should be used cautiously as typical peak-power meters can have SWR's as poor as 1.7:1. (A 1.7:1 meter SWR would produce a 0.3 dB difference between (2) and (3).)

As a final note on two-port de-embedding, (1) does have an alternate expression which might be of use to the reader in some instances. Recognizing that the input reflection coefficient of a two-port network is

$$\Gamma_{in} = S_{11} + \frac{S_{12}S_{21}\Gamma_L}{1 - S_{22}\Gamma_L} \tag{4}$$

Then, a little complex algebra shows that (1) can be rewritten as

$$\frac{P_1}{P_2} = \frac{|1-\Gamma_L S_{22}|\ (1-|\Gamma_{in}|^2)}{|S_{21}|^2\ (1-|\Gamma_L|^2)} \tag{5}$$

The above expression is much simpler than (1), but more connections are required in making the needed measurements. (Γ_{in} is an S_{11} measurement made with the load connected.)

Three-port de-embedding. Figure 2(b) illustrates the S-parameter flow diagram for a three-port network with no direct path between ports 2 and 3. Applying the diagram to the tester application (de-embedding the channel 1 peak-power measurements), port 2 corresponds to the radar port, and port 3 corresponds to the power-meter port. Again, applying Mason's technique to the flow diagram, the desired de-embedding expression is found to be

$$\frac{P_2}{P_3} = \frac{|S_{21}|^2|1-S_{33}\Gamma_{L3}|^2(1-|\Gamma_{L2}|^2)}{|S_{31}|^2|1-S_{22}\Gamma_{L2}|^2(1-|\Gamma_{L3}|^2)} \tag{6}$$

The most probable approximation to (6) is for the case of a three-port network with good output return losses (S_{22} and/or S_{33} are small). Additional approximations are possible if either the power meter or DUT have near ideal reflection coefficients (Γ_{L2} and/or Γ_{L3} are small). Regardless of the resulting approximation, the exact expression of (6) is valuable because it allows the designer to quantify the approximation's error.

Noise Figure De-Embedding

The block diagram of Figure 1 illustrates that the tester measures noise figure from the rear panel access links. Thus, to de-embed noise figure, the tester must account for the effects of both pre- and post-DUT loss. The HP 8970B noise figure meter includes the following features for de-embedding its noise figure measurements: 1) the effect of post-DUT loss is removable via instrument calibration; 2) the effect of pre-DUT loss is removable via a special function that requires the operator to enter the amount of pre-DUT loss, as well as its temperature. Implementation of the first feature in the tester requires only that the tester calibrate the noise figure meter through the post-DUT loss. Implementation of the second feature requires that the pre-DUT loss be measured as part of the tester's calibration. As in measuring loss for peak-power de-embedding, maximum accuracy dictates that the loss be measured in the proper manner.

The two equations the noise figure meter uses to correct its readings are

$$NF_{tot} = NF_1 + (NF_2-1)/G_1 + (NF_3-1)/G_1G_2 \qquad (7)$$

and

$$NF_1 = 1 + T_1/T_o(1/G_1 - 1) \qquad (8)$$

In this instance, NF_1 is the noise figure of the pre-DUT loss, NF_2 is the noise figure of the DUT, NF_3 is the noise figure of the post-DUT loss, and G_i refers to the corresponding gains/losses. In solving for NF_2, the operator influences the meter's accuracy via the value he enters for the pre-DUT loss (G_1). However, a subtle point which is often overlooked is that the variable "G" in (7) and (8) refers to a special kind of gain known as "available gain." (Available gain, for a two port network, is defined as the ratio of the power available from the network to the power available from the source.)

As previously illustrated, the various types of gains/losses can be expressed in terms of S-parameters via the application of Mason's loop rule to an appropriate flow diagram. The expression for the available gain of a two-port network turns out to be

$$G_a = \frac{(1-|\Gamma_s|^2)|S_{21}|^2}{|1-S_{11}\Gamma_s|^2 - |S_{22}(1-S_{11}\Gamma_s) + S_{21}S_{12}\Gamma_s|^2} \qquad (9)$$

Thus, the loss (G_1) one should enter into the noise figure meter

can be determined by measuring all four S-parameters of the pre-DUT loss, as well as the noise source reflection coefficient (Γ_s), and substituting these values into (9).

As was found to be the case in peak-power measurement de-embedding, the expression for available gain has both an alternate form and a more usable approximation. The alternate form, which involves an output reflection coefficient, is

$$G_a = \frac{1-|\Gamma_s|^2 \; |S_{21}|^2}{|1-\Gamma_s S_{11}|^2 \; (1-|\Gamma_{out}|^2)} \qquad (10)$$

The obvious approximation which (9) suggests is for the case where the noise source presents a good match (Γ_s is small). The resulting expression is simply

$$G_a = |S_{21}|^2/(1-|S_{22}|^2) \qquad (11)$$

However, this approximation is not universally valid, and should be used with caution, as typical microwave noise sources can have SWR's as poor as 1.35:1 ($|\Gamma_s| = 0.15$).

Besides the approximation, there is one other alternative method for measuring the pre-DUT loss that is very convenient. A secondary capability of all noise figure meters is the ability to measure small signal insertion gain. Thus, the noise figure meter itself would be able to measure the pre-DUT loss by simply removing the DUT from the measurement path. The primary source of error in using this technique is usually the fact that the meter measures insertion gain rather than available gain. The error introduced by the improper gain measurement can be expressed via the flow graph/loop-rule technique; the resulting expression is

$$\frac{G_a}{G_i} = \frac{(1-|\Gamma_s|^2) \; |1-\Gamma_L\Gamma_{out}|^2}{(1-|\Gamma_{out}|^2) \; |1-\Gamma_L\Gamma_s|^2} \qquad (12)$$

In this case, Γ_L is the reflection coefficient of the DUT's input port. As an example of the type of gain errors possible, consider the case-- admittedly oversimplified-- where all of the Γ's in (12) have a magnitude of 0.15 (SWR=1.35:1). Then (12), the resulting gain error, would range anywhere from -0.4 dB to +0.4 dB. The effect such a gain error would have on de-embedded noise figure is a function of the net system gain and can be calculated from (7).

Conclusions/Summary

This paper was written from both a specific and general point of view. The discussion on the tester's instrument integration included an actual block diagram of the Sandia tester; this was done to provide a specific example of how the HP 85110A's access

links can be utilized. On the other hand, the de-embedding discussion and analysis was carried out from a general point of view to be of maximum service to the reader: the expression one should use to de-embed a measurement is ultimately a function of the measurement environment and the accuracy desired. For example, the usefulness of some of the approximations was shown to be a function of the instrument's reflection coefficient at the measurement frequency.

In concluding this paper, it is appropriate to provide the reader with some brief information on the tester's software. The complexity of testing a T/R module requires that the software do much more than just control instruments. For example, the software's phase analysis capabilities include polynomial curve fitting algorithms which allow the module's phase linearity to be characterized (i.e., cubic/quadratic phase error). Another aspect of the software is that it performs a significant amount of data "crunching". For example, because a module's phase accuracy is a function of temperature, bias level, RF drive level, and module phase-state, the Sandia tester takes phase measurements at over 5000 permutations of these variables. The software must then analyze this phase information and output the results in a concise, usable format.

The tester's use of the Maury tuners also requires some explanation. The tester uses the tuners to provide an all-phase, constant-SWR load-pull. Because this is not an application which is supported by the manufacturer, custom software had to be written by Sandia to enable the tuners to perform this task. This software development was complicated by the fact that the tuners are not linear; thus, in addition to the controlling software, a custom characterization algorithm also had to be developed.

The reader should also be aware that in addition to the major instruments, the tester also includes several ancillary instruments such as a pulse generator, data generator, programmable power supply, and a temperature chuck. (The pulse/data generators are used for providing control signals to the T/R module.) In addition, the tester includes a second test set, which is the 8510's original CW-mode 8514A. This test set is used to characterize the 85110A for measurement de-embedding.

In summary, the success of the Sandia tester is a result of the custom application and integration of a diverse collection of state-of-the-art test equipment. This results in a T/R module test system that achieves a single-connection test capability without sacrificing measurement sophistication or accuracy.

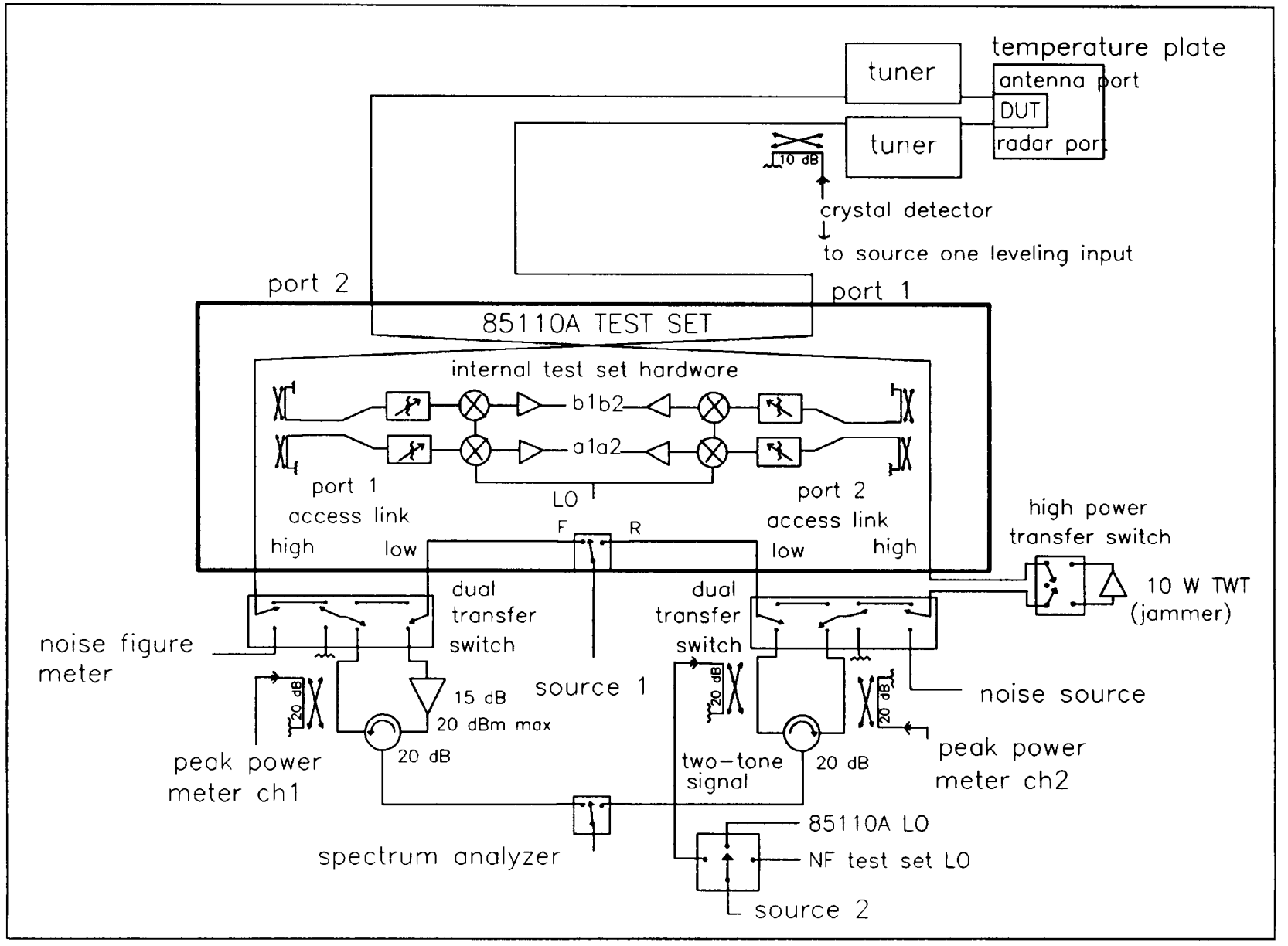

Figure 1. Block diagram of test set interconnections

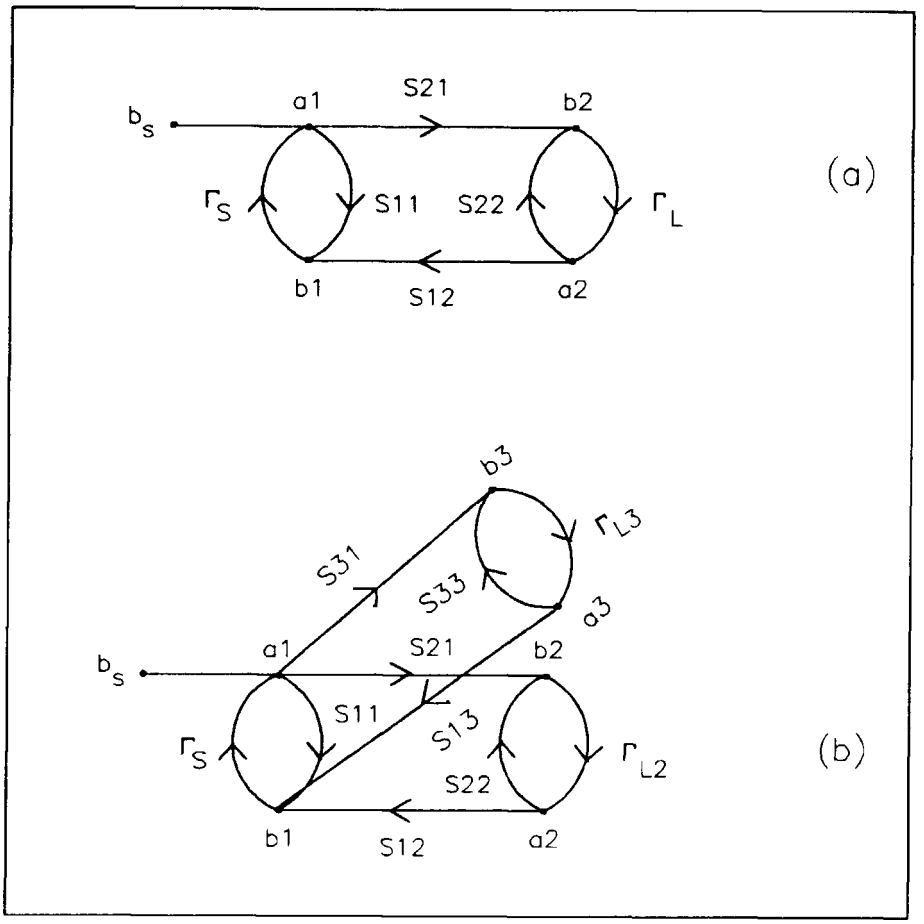

Figure 2. S-parameter flow diagrams. (a) Two-port network. (b) Three-port network.

DISCLAIMER